Quantitative proteomics analysis using 2D-PAGE to investigate the effects of cigarette smoke and aerosol of a prototypic modified risk tobacco product on the lung proteome in C57BL/6 mice

Ashraf Elamin [a,1], Bjoern Titz [a,1], Sophie Dijon [a,1], Celine Merg [a], Marcel Geertz [a,d], Thomas Schneider [a], Florian Martin [a], Walter K. Schlage [c], Stefan Frentzel [a], Fabio Talamo [a], Blaine Phillips [b], Emilija Veljkovic [b], Nikolai V. Ivanov [a], Patrick Vanscheeuwijck [a], Manuel C. Peitsch [a], Julia Hoeng [a,*]

[a] Philip Morris Research and Development, Philip Morris Products SA (part of Philip Morris International group of companies), Quai Jeanrenaud 5, 2000 Neuchâtel, Switzerland
[b] Philip Morris International Research Laboratories (part of Philip Morris International group of companies), 50 Science Park Road, 117406, Singapore
[c] Biology Consultant, Max-Baermann-Str. 21, 51429, Bergisch Gladbach, Germany
[d] Bayer Technology Services GmbH, 51368 Leverkusen, Germany

ARTICLE INFO

ABSTRACT

Smoking is associated with several serious diseases, such as lung cancer and chronic obstructive pulmonary disease (COPD). Within our systems toxicology framework, we are assessing whether potential modified risk tobacco products (MRTP) can reduce smoking-related health risks compared to conventional cigarettes. In this article, we evaluated to what extent 2D-PAGE/MALDI MS/MS (2D-PAGE) can complement the iTRAQ LC-MS/MS results from a previously reported mouse inhalation study, in which we assessed a prototypic MRTP (pMRTP). Selected differentially expressed proteins identified by both LC-MS/MS and 2D-PAGE approaches were further verified using reverse-phase protein microarrays. LC-MS/MS captured the effects of cigarette smoke (CS) on the lung proteome more comprehensively than 2D-PAGE. However, an integrated analysis of both proteomics data sets showed that 2D-PAGE data complement the LC-MS/MS results by supporting the overall trend of lower effects of pMRTP aerosol than CS on the lung proteome. Biological effects of CS exposure supported by both methods included increases in immune-related, surfactant metabolism, proteasome, and actin cytoskeleton protein clusters. Overall, while 2D-PAGE has its value, especially as a complementary method for the analysis of effects on intact proteins, LC-MS/MS approaches will likely be the method of choice for proteome analysis in systems toxicology investigations.

Significance: Quantitative proteomics is anticipated to play a growing role within systems toxicology assessment frameworks in the future. To further understand how different proteomics technologies can contribute to toxicity assessment, we conducted a quantitative proteomics analysis using 2D-PAGE and isobaric tag-based LC-MS/MS approaches and compared the results produced from the 2 approaches. Using a prototypic modified risk tobacco product (pMRTP) as our test item, we show compared with cigarette smoke, how 2D-PAGE results can complement and support LC-MS/MS data, demonstrating the much lower effects of pMRTP aerosol than cigarette smoke on the mouse lung proteome. The combined analysis of 2D-PAGE and LC-MS/MS data identified an effect of cigarette smoke on the proteasome and actin cytoskeleton in the lung.

1. Introduction

Smoking is the cause of several serious diseases such as lung cancer, cardiovascular disease and chronic obstructive pulmonary diseases. Smoking cessation is the best option for smokers to reduce the risk for adverse health outcomes. For smokers who otherwise would not quit, switching to less hazardous products provides an alternative way to reduce the harm from smoking-related diseases. In this context, a modified risk tobacco product (MRTP) is defined as "any tobacco product that is sold or distributed for use to reduce harm or the risk of tobacco-related disease associated with commercially marketed tobacco products" [1]. Combustion of organic tobacco compounds at elevated temperatures has been identified as the major source of the harmful or potentially harmful constituents (HPHCs) of cigarette smoke, as most HPHCs are produced through pyrolysis and pyrosynthesis [2–6].

This fact forms the basis for the development of MRTPs that rely on the *heat-not-burn* concept and prevent combustion processes by applying lower, well-controlled temperatures for the generation of an aerosol with a significantly reduced content of HPHCs compared with cigarette smoke (e.g., [2,7,8]). For one of the prototypic MRTP (pMRTP), developed by Philip Morris International and tested in two previously conducted in vivo studies, this is achieved with a carbon tip attached to a column of tobacco filler; the tip serves as a heat source to generate an aerosol [8,9].

To assess the biological effects of potential MRTPs, we are conducting studies engaging a systems toxicology approach that combines evaluation of classical toxicological endpoints with extensive molecular measurements and computational analysis approaches [10]. The aim is to provide a deeper mechanistic understanding of the induced biological effects, toward a more robust and sensitive detection of these effects. To achieve this, we routinely combine different "omics" measurement techniques to capture how the transcriptome, proteome and lipidome of various rodent's organs including lungs, a target organ for smoke related pathologies, are affected by the exposure conditions [8, 11]. For the proteomics analyses, we have established a robust LC-MS/MS workflow using isobaric tag-based quantification (iTRAQ® or TMT™) that allows for multiplexed analyses and supports the quantitative assessment of several molecular processes in lung tissue known to be affected by CS exposure (xenobiotic, oxidative stress, metabolic, and immune responses) (e.g., [7,8,11–13]). However, proteomics methods based on 2D-PAGE/Matrix Assisted Laser Desorption Ionization (MALDI) MS/MS have been the centerpiece of toxicoproteomics for a long time and provide a complementary way to analyze proteomes, as they are based on the separation of intact proteins rather than cleaved peptides (as in our LC-MS/MS workflow [14,15]). While a few direct comparisons between LC-MS/MS and 2D-PAGE/MALDI MS/MS workflows are available (e.g., [16]), our question was to what extent 2D-PAGE/MALDI MS/MS results can complement LC-MS/MS results in the context of systems toxicology studies.

In this article, we compared quantitative lung proteomics results from 2D-PAGE and iTRAQ-based LC-MS/MS analyses from a 7-month mouse inhalation study on C57BL/6 mice, which has been previously published, including the iTRAQ results only [8,11]. In this inhalation study, we compared the biological effects of exposures to CS, aerosol of a prototypic MRTP (pMRTP), switching from CS to pMRTP aerosol and cessation. Consistent with previous reports, we found that the iTRAQ-based workflow provides a larger coverage of the exposure effects than 2D-PAGE. Nevertheless, the 2D-PAGE results complement the iTRAQ results by reconfirming the general trends and supporting the identification of specific protein clusters affected by CS exposure.

2. Materials and methods

2.1. Experimental design

The study included five groups of mice, exposed as follows: 1. sham (exposed to filtered fresh air); 2. CS (exposed to mainstream smoke from 3R4F, a reference cigarette from the University of Kentucky); 3. pMRTP (exposed to aerosol from the prototypic MRTP); 4. smoking cessation (CS followed by smoking cessation); and 5. switching to pMRTP (CS followed by pMRTP). C57BL/6 mice were exposed as indicated for up to 7 months. To model the effects of smoking cessation and switching to the pMRTP, groups of mice were first exposed to CS for 2 months and exposure was then changed to filtered air (cessation) or pMRTP (switching) for an additional 5 months. The 2-month time point for switching/cessation was chosen based on the results of a previously conducted inhalation study on C57BL/6 mice, which had indicated that lung inflammation, emphysema, and changed pulmonary function were already apparent after 2 months of exposure to 3R4F [17]. Lung tissue samples for proteomics analysis were collected after 1, 3, 5, and 7 months of exposure – an additional 4 month time point was analyzed

by a reverse phase protein array (RPPA). Each C57BL/6 group at each sample collection point included six mice (six biological replicates) for the 2D-PAGE analysis and ten mice (ten biological replicates) for the RPPA analysis.

For additional details on the endpoints of this 7-month C57BL/6 mouse inhalation study, the reader is referred to Phillips et al. [8] and [18]. The iTRAQ® analysis was performed in six biological replicates. For more details on the iTRAQ® analysis see Titz et al. [11] and the Supplementary Text.

2.2. Animals

All procedures involving animals were approved by an Institutional Animal Care and Use Committee, in compliance with the National Advisory Committee for Laboratory Animal Research (NACLAR) Guidelines on the Care and Use of Animals for Scientific Purposes. In accordance with the "3Rs" principles of animal research (replacement, reduction and refinement), we used the minimum number of animals needed to obtain valid results and the least invasive procedures to minimize pain and distress. Our laboratory technicians and veterinary specialists are trained in the latest techniques to most effectively and humanely manage and care for animals.

Female C57BL/6 mice bred under specific pathogen-free conditions were obtained from Charles River, Wilmington, MA, USA. The mice were 8–10 weeks old at the start of exposure. See Ansari et al. [18] for more details and for an overview of the number of animals assigned to the different endpoints of the study.

2.3. Reference cigarettes and pMRTP

3R4F cigarettes were purchased from the University of Kentucky (Lexington, KY, USA; http://www.ca.uky.edu/refcig). pMRTP (Philip Morris Products S.A., Neuchâtel, Switzerland) has a carbon tip attached to a tobacco plug that serves as a fast-lighting heat source to generate an aerosol. With this, the temperature applied to the tobacco plug is below the combustion temperature. This technology, by avoiding tobacco combustion, reduces formation of HPHCs [8].

2.4. Smoke generation and animal exposure

Mainstream CS from 3R4F cigarettes was generated on a 30-port rotary smoking machine (type PMRL-G, SM2000) as described previously [8,9]. pMRTP aerosol was generated in modified SM2000 machines. 3R4F cigarettes and pMRTP sticks were smoked according to the Health Canada Intensive Smoking Protocol based on ISO standard 3308 (revised in 2000), with the exception of the puff volume (55 mL) and puff frequency (one puff every 30 s), as described previously [8]. Several additional minor deviations from ISO standard 3308 were necessary for technical reasons [8]. Aerosols were diluted with conditioned fresh air to achieve the target concentrations.

The C57BL/6 mice were whole body-exposed to diluted mainstream smoke from 3R4F cigarettes (750 mg TPM/m³, equivalent to 34.4 mg nicotine/m³), pMRTP aerosol (nicotine-matched to 3R4F, 34.4 mg/m³), or filtered air, for 4 h per day, 5 days per week, for up to 7 months, with intermittent daily exposure to fresh filtered air for 30 min after the first hour of smoke exposure and for 60 min after the second and third hours of exposure. Mice exposed only to fresh air served as the control (sham) group. Reproducibility of smoke generation was ensured by periodic analysis of the test atmosphere during the study, and reliable exposure of the mice was verified by a number of biomarkers (see [8] for details).

2.5. 2D-PAGE

The TissueLyser II (Qiagen, Hilden, Germany) bead-mill disruption system was used for protein extraction from cryo-sliced right lung

tissue samples (6 biological replicates). Protein extraction was performed according to the manufacturer's instructions, using one 5-mm steel bead (Qiagen) and 1 mL of lysis buffer ReadyPrep 2D Protein Extraction Kit (Total) (7 M urea, 2 M thiourea, 1% (w/v) Amidosulfobetaine-14, 40 mM Tris base, and 0.001% Bromophenol Blue, Biorad) completed with (v/v) 1% Tributylphosphine, (v/v) 10% Ethanol HPLC Grade (Sigma Aldrich), (v/v) 0.5% Protease inhibitor (protease inhibitor, GE Healthcare) and (1tab/10 mL) Phosphatase inhibitor (PhosSTOP, Roche). After a centrifugation for 10 min at 16 000 ×g, the supernatant was collected in a fresh tube then underwent an acetone-precipitation. The precipitated sample was resuspended in ReadyPrep 2D Starter kit rehydration/sample buffer (8 M urea, 2% 3-[(3-cholamidopropyl)dimethylammonio]-1-propanesulfonate, 50 mM dithiothreitol, 0.2% Bio-lyte ampholytes pH gradient buffer pH 3–10, and bromophenol blue; BioRad). The protein concentration was determined using the modified Bradford protein assay (BioRad).

Isoelectric focusing was performed using 250 μg of proteins on 11-cm immobilized pH gradient strips (Readystrip IPG strip 3–10NL, BioRad) with a pH 3–10 nonlinear gradient, on an Ettan IPGphor System (GE Healthcare, Little Chalfont, UK). The proteins bound to the strips were reduced and alkylated before separation in a second dimension using a Criterion XT Bis-Tris Gel, 12%, 13.3 × 8.7 cm (W × L) (BioRad). For image analysis, the gels were visualized with SYPRO Ruby staining (Invitrogen, Carlsbad, CA, USA). After scanning of the gels, spot-intensity calibration, spot detection, background abstraction, and matching of 2D-PAGE were performed on the digitized images using SameSpots software (Nonlinear, Newcastle upon Tyne, UK). The comparative analyses of all gels was based only on the spots detected at month 7 so as to apply the same set throughout the four time points. For the detection of differentially expressed proteins (exposure vs. sham), the values were log transformed, a linear model was fit for each exposure condition and its respective sham group (from the same time point), and p-values from a moderated t-statistics were calculated with the empirical Bayes approach [19]. The Benjamini-Hochberg false discovery rate (fdr) method was then used to correct for multiple testing effects. Proteins with an fdr-adjusted p-value <0.05 were considered as differentially expressed.

For identification, protein spots were excised from the gels, followed by washing and in-gel digestion with 20 ng of Trypsin Gold, Mass Spectrometry Grade (Promega, Madison, WI, USA) using an ETTAN digester robot (GE Healthcare). The extracted tryptic peptides were mixed with cyano-4-hydroxycinnamic acid matrix (Bruker, Bremen, Germany) and deposited on a MALDI target plate to be analyzed. Peptide mass fingerprint data and mass spectra were acquired by MALDI time-of-flight mass spectrometry (UltraFleXtreme MALDI-TOF/TOF-MS; Bruker) and identified with the MASCOT search program and the SwissProt database (Taxonomy: *Mus musculus*, Enzyme: Trypsin, Missed cleavages ≤2, Global modifications: Oxidation (M), Variable modifications: Carbamidomethylation (C), MS tolerance: 100 ppm, MS/MS Tolerance: 0.7 Da).

2.6. Reverse-phase protein array (RPPA) analysis

The TissueLyser II (Qiagen, Hilden, Germany) bead-mill disruption system was used for protein extraction from cryo-sliced right lung tissue samples of ten mice. Protein extraction was performed according to the manufacturer's instructions, using one 5-mm steel bead (Qiagen) and 400 μL CLB1 extraction buffer (Bayer Technology Services GmbH, Leverkusen, Germany). After extraction, the samples were centrifuged in a microcentrifuge for 10 min at 11,000 ×g, and the supernatant was transferred into fresh tubes for further analysis. Protein concentration in collected supernatants was quantified using an EZQ test (Life Technologies, Carlsbad, CA, USA). Protein extracts were stored at −80 °C until further use.

Analysis of protein extracts by Zeptosens® RPPA technology was performed as previously described [20]. Protein extracts were diluted with CLB1 buffer to a final spotting concentration of 0.2 μg/μL. Diluted

extracts were printed at four serial dilutions (1.6-fold) onto Zeptosens® hydrophobic chips (Bayer Technology Services GmbH) using a microarray printer (NanoPlotter 2.1, GeSiM, Grosserkmannsdorf, Germany). Each sample was processed in technical duplicate with independent dilutions on separate arrays, i.e., eight spots per sample with four spots per array. Following array printing, arrays were blocked, washed, and dried according to the manufacturer's specifications and stored at 4 °C in the dark until use.

For measurement of protein signals, arrays were incubated overnight at room temperature in primary antibodies at dilutions of 1:500 in CAB1 assay buffer (Bayer Technology Services GmbH). The following primary antibodies were used: Chi3l1 (#sc-30861, Santa Cruz Biotechnology, Dallas, TX, USA), Actb (#4970, Cell Signaling Technology, Danvers, MA, USA), Ctsd (#TA301315, Origene, Rockville, MD, USA), Vim (#LS-B4669, LSBio, Seattle, WA, USA), Asah1 (#ARP57760_P050, Aviva Systems Biology, San Diego, CA, USA), Capg (#sc-33084, Santa Cruz Biotechnology), Psma5 (#TA310789, Origene), Capzb (#AB6017, Merck Millipore, Darmstadt, Germany), and Sftpa (#sc-13977, Santa Cruz Biotechnology). Following washing, arrays were incubated for 2 h with either Alexa647- (Life Technologies) or Dylight650- (Bio-Rad AbD Serotec GmbH, Puchheim, Germany) labeled anti-species secondary antibodies at dilutions of 1:500. After subsequent washing, stained arrays were imaged using an array scanner (ZeptoREADER, Bayer Technology Services GmbH) according to the manufacturer's recommendations. For correction for secondary antibody staining, arrays were assayed in the absence of primary antibodies. For measurement of spotted protein amounts, one blank chip (i.e., without antibody incubation) was stained with SYPRO® Ruby. Scanned images were analyzed using ZeptoVIEW 3.1 software (Bayer Technology Services GmbH). Normalized fluorescence intensity (NFI) for each sample and protein target were calculated as reference fluorescence intensities of primary antibody stained arrays (RFIprimary) corrected for secondary antibody staining (RFIsecondary), as well as relative spotted protein concentration (RFIprotein), determined by (RFIprimary − RFIsecondary)/RFIprotein, using the ZeptoVIEW 3.1 software. NFI values were used for subsequent analysis. Statistics was based on t-tests of log-transformed data; only comparisons with at least three not missing values per group considered. The Benjamini-Hochberg false discovery rate (fdr) method was then used to correct for multiple testing effects. Proteins with an fdr-adjusted p-value <0.05 were considered as differentially expressed.

2.7. Additional data analysis methods

For the comparison of 2D-PAGE and iTRAQ data, gene set analysis (GSA) was conducted with the Piano package in the R statistical environment [21]. Gene sets were defined based on the differentially expressed proteins from the 2D-PAGE analysis. GSA of these sets was performed for each comparison of the iTRAQ data, fold-change was used as the gene/protein statistic, the mean of the fold-changes as the set statistic, and gene/protein permutation with false-discovery rate correction of the obtained p-values to estimate significance. Functional associations among proteins were obtained from the STRING database [22]. Functional clusters were identified using an information-theoretic algorithm [23] and manually annotated guided by ToppGene [24].

2.8. Data availability

The 2D-PAGE data are available from figshare (see [18]). The iTRAQ mass spectrometry proteomics data are available from the ProteomeXchange Consortium via the PRIDE partner repository (http://www.ebi.ac.uk/pride/archive/) [25]. The database identifier is PXD001369.

3. Results

3.1. Design of 7-month mouse exposure study with multiple proteomics endpoints

The lung proteomics results presented here are part of a larger systems toxicology assessment study of pMRTP, a prototypic MRTP [8,18], and we have already published an integrative analysis of the iTRAQ-based quantitative lung proteomics data [11]. The current manuscript focuses on the results from 2D-PAGE analysis of the lung proteome, comparison and integration with the iTRAQ data, and further verification of selected differentially expressed proteins using RPPA.

Briefly, C57BL/6 mice were exposed for up to 7 months to filtered air (sham), CS from the 3R4F reference cigarette (3R4F), or aerosol from the pMRTP (Fig. 1A). In addition, cessation and switching groups were first exposed to 3R4F CS for 2 months and subsequently to fresh air and pMRTP aerosol, respectively. Importantly, the pMRTP aerosol exposure was matched in nicotine concentration to the 3R4F CS exposure. Effective and robust exposure conditions including comparable nicotine uptake were confirmed and the results are summarized in Phillips et al. [8].

3.2. 2D-PAGE captures exposure response of the lung proteome

To measure the response of the lung proteome, tissue samples taken at the end of months 1, 3, 5, and 7 were analyzed. These samples were analyzed by 2D-PAGE using separation by isoelectric focusing on 11-cm immobilized pH gradient strips (pH 3–10, nonlinear gradient) and, subsequently, by SDS-PAGE. Protein spots were stained with SYPRO Ruby, quantified, then identified (Fig. 1B, C).

First, we compared the amplitude (fold-changes) and statistical significance of the effects (Fig. 2A, Supplementary Table 1). 3R4F CS clearly induced changes in the lung proteome that appeared to increase over time – with the highest number of protein spots identified above the significance threshold (fdr-adjusted p-value <0.05) for month 7. In contrast, pMRTP aerosol exposure did not result in statistically significant effects on the lung proteome compared with the respective sham groups as measured by 2D-PAGE. Differential protein expressions in

the cessation and switching groups appeared to return quickly to sham group levels. The numbers of proteins (i.e., protein spots) with statistically significant differential abundance (fdr-adjusted p-value <0.05) are summarized in Fig. 2B. Note that for some protein spots with differential abundance, the proteins could not be identified.

In total, we were able to identify 20 protein spots (mapped to 17 proteins) with differential abundance, of which 17 demonstrated up-regulation compared with the sham group (Fig. 2C). Overall, these proteins showed similar response profiles with the largest effect after 7 months of 3R4F exposure, low to absent effects after pMRTP aerosol exposure, and a tendency to still be affected in samples taken at the first cessation or switching time point, i.e., 1 month after switching/cessation. Examples of the 2D-PAGE spot intensities for proteins Ctsd and Fabp5 are shown in Fig. 2D and E.

3.3. Comparison of 2D-PAGE and iTRAQ lung proteome response profiles

We have already reported on the lung proteome results of this study obtained with the iTRAQ isobaric labeling approach [8,11]. Using iTRAQ, 4347 proteins (protein groups) were identified. However, of these only about 2000 proteins were consistently identified in at least two-thirds of the replicates and used for quantitative assessment (Fig. 3A). Using the 2D-PAGE approach, we identified more than 1500 protein spots consistently across all samples, because we used the same quantification mask for all gels (see Section 2).

While, overall, the 2D-PAGE approach confirmed the differences in the lung proteome response between 3R4F CS exposure, pMRTP aerosol exposure, switching, and cessation, a lower number of proteins were identified as differentially abundant as compared to iTRAQ experiments – e.g., for 7 months of 3R4F vs. sham exposure ~700 differentially expressed proteins (DEPs) were identified by iTRAQ and ~50 DEPs were identified by 2D-PAGE (Fig. 3A). The differences were likely attributed to the higher variance in 2D-PAGE and lower separation power as compared to the iTRAQ data (Supplementary Fig. 1).

To assess the similarity between the proteome response detected by 2D-PAGE and iTRAQ, we conducted a set enrichment analysis across the two data types (Fig. 3B). With this, we tested whether the sets of up- or down-regulated proteins identified by 2D-PAGE were also differentially
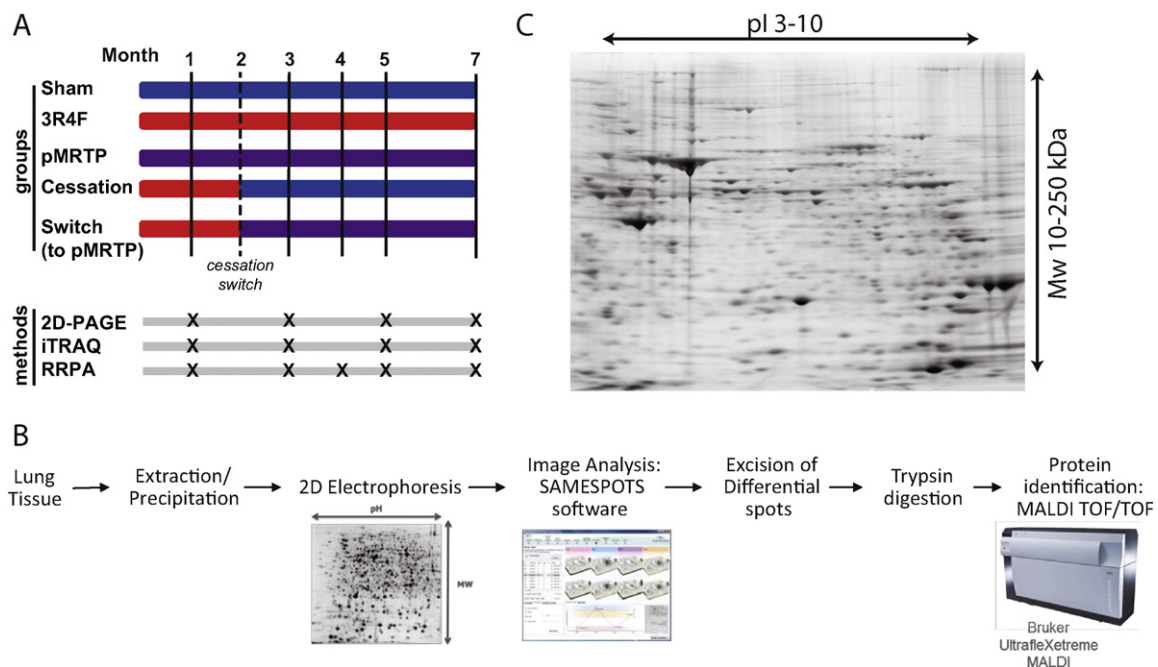

Fig. 1. Design of 7-month CS exposure study and 2D-PAGE workflow. (A) Schematic of the study design and sampling time points. C57BL/6 mice were exposed to cigarette smoke (3R4F), a prototypic modified risk product (pMRTP) or fresh air (sham). Some mice were exposed to CS for 2 months and then either underwent cessation or were switched to pMRTP aerosol. Lung tissue samples for 2D-PAGE, iTRAQ, and RPPA were collected at the indicated time points. (B) Workflow of 2D-PAGE experiment. (C) Representative example of a stained 2D gel.
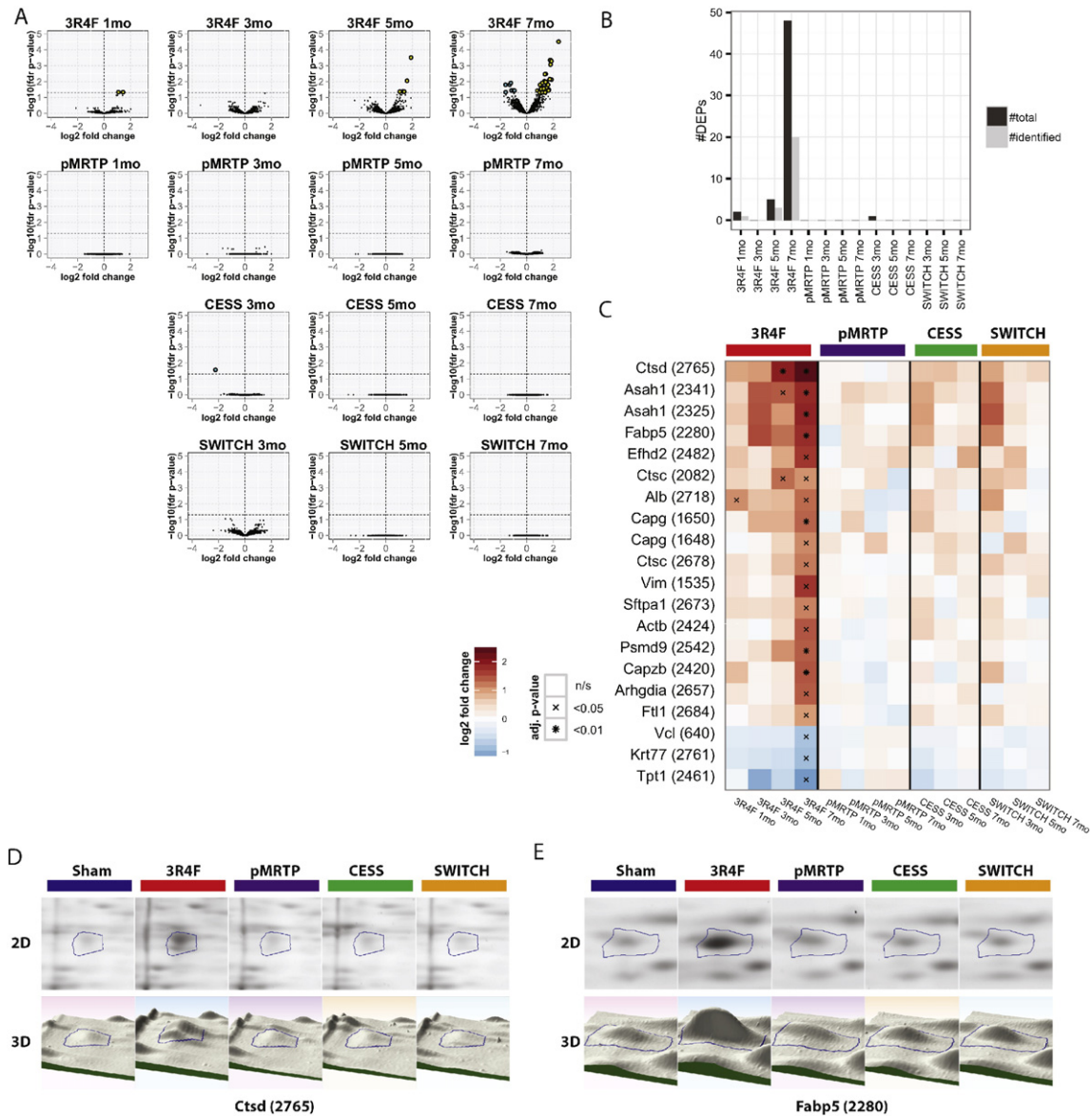
Fig. 2. 2D-PAGE captures the lung proteome response to CS and pMRTP exposure. (A) Volcano plots showing the effect amplitude (log$_2$ fold-change, x-axis) and significance ($-\log_{10}$ adjusted p-value, y-axis) in the exposure groups compared with sham exposure. The significance threshold of the fdr-adjusted p-value = 0.05 (1.3 in log$_{10}$ space) is indicated and significantly up and downregulated proteins (protein spots) detected by 2D-PAGE are shown as yellow and blue dots, respectively. (B) Summary of the number of detected differentially expressed proteins (DEPs) in total and that could be identified by MALDI-TOF. (C) Protein response heatmap for all identified proteins with significant differential expression by 2D-PAGE (fdr-adjusted p-value < 0.05). Each row represents a protein spot (labeled with protein name and spot number), each column represents an exposure group vs. sham comparison. The log$_2$ fold-change is color-coded (see color key) and the statistical significance indicated ($\times$ = adj. p < 0.05; * = adj. p < 0.01). Note that for the basic statistics we counted different protein spots for the same proteins separately. (D) Representative spot intensities of protein Ctsd (spot #2765) for one replicate of the 7 month time point (2D- and 3D- representation). (E) As D, but for Fabp5 (spot #2280).

regulated in the iTRAQ data. Indeed, protein sets that were detected as significantly upregulated by 2D-PAGE showed a significant association specifically with the upregulated proteins in the iTRAQ data set upon 3R4F exposure, as well as with those identified at the first time points after cessation/switching.

For comparison of individual protein responses, we focused on the 7-month 3R4F vs. sham exposure data, which showed the largest number of differentially expressed proteins by 2D-PAGE (Fig. 3C). For this, only proteins with significant differential expression identified by either method were considered. Of the 17 differentially expressed proteins in the 2D-PAGE data, 11 were also significantly differentially expressed in the iTRAQ data, and only a single protein (Tpt1) showed a significant conflicting directionality between the data types. Of note, this plot highlights the ability of 2D-PAGE to separate protein species. For example, only one out of three detected Ctsd species was significantly increased

in the 2D-PAGE data. Finally, we compared the iTRAQ fold-change distributions and found a clear right shift (toward higher fold-changes) of the upregulated proteins detected by 2D-PAGE, with Ctsd and Fabp5 among the most highly upregulated proteins upon 3R4F exposure in the iTRAQ data (Fig. 3D).

In summary, while under these conditions 2D-PAGE demonstrated less sensitivity than iTRAQ, the results were consistent overall and the 2D-PAGE results confirmed the response profiles previously reported from the iTRAQ (and transcriptomics) data [8, 11].

3.4. Functional network embedding for augmented data interpretation

The low number of identified and differentially abundant proteins in the 2D-PAGE data created challenges for biological interpretation beyond the level of individual proteins. Therefore, we leveraged a
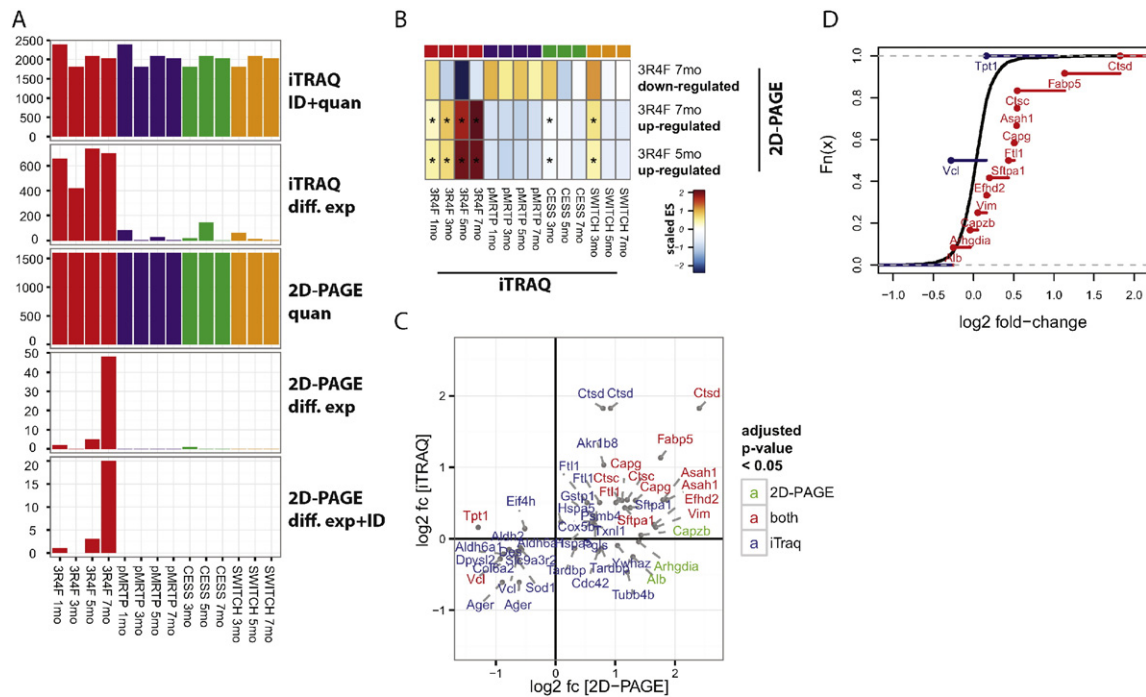
Fig. 3. Comparison of proteome response profiles measured by 2D-PAGE and iTRAQ. (A) Comparison of the number of identified, quantified, and differentially expressed proteins measured by 2D-PAGE and iTRAQ. From top to bottom, the bar chart shows for each exposure group vs. sham comparison: the number of identified and reliably quantified proteins from iTRAQ (see Methods), the number of differentially expressed proteins identified by iTRAQ (fdr-adj. *p*-value < 0.05), the number of quantified protein spots from 2D-PAGE, the number of differentially expressed protein spots from 2D-PAGE, and the number of differentially expressed protein spots to which a protein identifier could be assigned. (B) Comparison of 2D-PAGE with iTRAQ differential expression results. Protein sets are defined based on the differentially expressed proteins from the 2D-PAGE analysis (3R4F 5 months upregulated, 3R4F 7 months up/downregulated). Gene/protein set analysis (GSA) of these sets was performed for each comparison of the iTRAQ data and the mean fold-change, scaled per gene set, was color coded (ES, enrichment score) and the statistical significance indicated (* = fdr-adjusted *p*-value <0.05). (C) Scatter plot comparing the fold-change responses of differentially expressed proteins from the 3R4F 7 months vs. sham comparison from 2D-PAGE and iTRAQ data. The color of the protein label indicates whether differential expression was identified by 2D-PAGE (green), iTRAQ (blue), or both (red). (D) Empirical cumulative density functions for all quantified proteins by iTRAQ for the 3R4F 7 months vs. sham comparison (black), for the proteins with significant upregulation by 2D-PAGE (red), and for proteins with significant downregulation by 2D-PAGE (blue).

functional association clustering approach combining both the 2D-PAGE and iTRAQ results (Fig. 4). The guiding idea was to embed the differentially expressed proteins identified by 2D-PAGE in larger functional clusters co-defined by the 2D-PAGE and iTRAQ results and then interpret the roles of the differentially expressed proteins (DEPs) identified in the 2D-PAGE data in this context. Importantly, if core components of these clusters are identified by both methods, this supports the biological relevance of these functional clusters. Again, we focused on the 7-month 3R4F vs. sham exposure comparison, which showed the largest number of differentially expressed proteins in the 2D-PAGE data; in particular, we focused on the group of 14 proteins upregulated upon 3R4F exposure.

In total, seven of the identified functional clusters contained differentially upregulated proteins in the 2D-PAGE data (Fig. 4, numbered clusters). Two clusters (12 and 13) were associated with the immune response (myeloid-associated proteins) and cluster 11 indicates an increase in surfactant metabolism—both effects have been described previously for this study and have been linked to an increase in immune cells and surfactant lipids, respectively [8,11]. Especially for clusters 11 and 12, the overall response is well supported by key nodes in these cluster networks that were measured by both iTRAQ and 2D-PAGE (Sftpa1 and Ctsd/Ctsc/Asah1). The 2D-PAGE data also supported the upregulation of an actin cytoskeleton-related cluster (3, through Capg/Actb/Arhgdia/Capzb/Efhd2) and a proteasome cluster (4, Psmd9).

All in all, by embedding the 2D-PAGE-defined DEPs in extended functional clusters, we were able to define the biological responses captured by 2D-PAGE, especially of immune-, surfactant-, actin cytoskeleton-, and proteasome-related processes that are induced by 3R4F CS exposure.

3.5. Measurement of key cluster nodes by reverse-phase protein array (RPPA)

Having further demonstrated that CS exposure affects specific functional protein clusters in mouse lung, we set up reverse-phase assays to target key components of these clusters (Fig. 5) to verify the detected response from 2D-PAGE and iTRAQ. Overall, the RPPA results were in agreement with the 2D-PAGE and iTRAQ results, i.e., they showed significant increases for the 3R4F exposure groups and limited effects upon pMRTP exposure and in the later samples from the cessation and switching groups.

4. Discussion

Systems toxicology complements the classical endpoints in toxicological studies by including more extensive measurements of the molecular effects caused by toxicant exposure [10]. The goal is to globally analyze the induced molecular changes in the context of their biological networks to derive deeper mechanistic insights for a given toxicant—toward more robust and more sensitive detection of toxicant effects and, eventually, to facilitate translation between different assessment systems and species. In addition, by supporting the (mechanism-based) translation between in vitro and in vivo systems and by providing more extensive insights from each animal for in vivo studies, systems toxicology approaches can be effective under the 3Rs principle, to refine, reduce, and eventually replace animal studies [26].

Toxicants have broad biological effects, for example, the measurement of their effects on the transcriptome, proteome, metabolome, and lipidome have contributed to the elucidation of toxicological effects
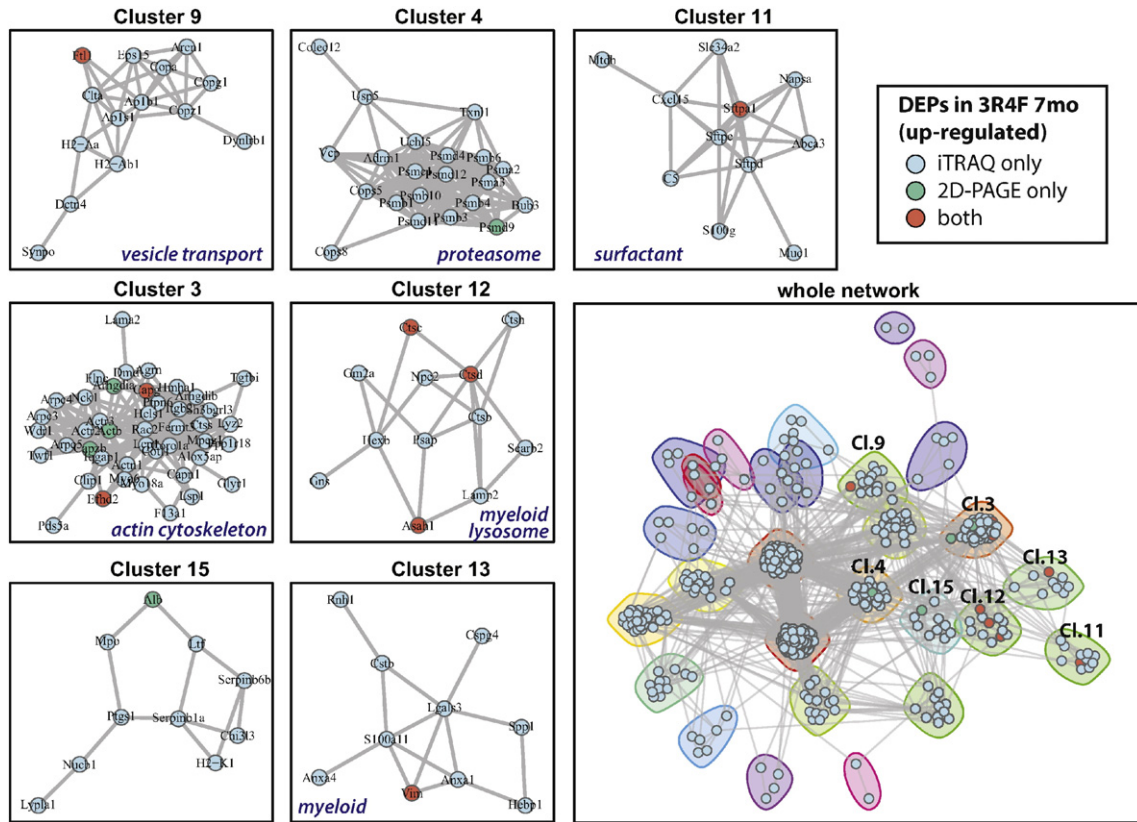
Fig. 4. Functional network embedding for interpretation of the detected exposure response (3R4F 7 months vs. sham). Functional association clusters were identified for the significantly upregulated proteins in the 2D-PAGE and iTRAQ data (3R4F 7 months vs. sham) (see whole network figure). Functional protein clusters are color-coded and clusters with differentially expressed proteins identified by 2D-PAGE are labeled. For each of these clusters, the association graph is shown and enriched biological functions are indicated.

and mechanisms [11,12,27–32]. Quantitative proteomics is an important component of our systems toxicology assessment strategy, as it quantitatively captures a broad range of disease-relevant effects of cigarette smoke exposure including the xenobiotic, oxidative stress, metabolic and inflammatory responses of lung tissue [8,11,12].

Several alternative technologies for the separation, identification and quantification of proteome alterations are available, each with their particular strengths and limitations. Bottom-up proteomics approaches that combine LC for peptide separation with tandem MS for identification and quantification (LC-MS/MS) are becoming increasingly popular because of improvements in instrumentation and quantification approaches [11,33,34]. Gel-based proteomics methods, especially

2D-gel based approaches, have been a robust "workhorse" for toxicoproteomics and are still in common use in toxicological investigations [12]. 2D-gel workflows have been compared with LC-MS/MS workflows previously. For example, Putz et al. compared results from a 2D-PAGE workflow and two LC-MS/MS-based workflows, using iTRAQ- or SILAC-based quantification, in a cell culture model of malignant transformation [16]. In these experiments, the iTRAQ workflow resulted in more identified differentially expressed proteins as compared to 2D-PAGE. Overall, the authors concluded that, while the methods provide complementary results, iTRAQ outperforms 2D-PAGE both in the number of identified proteins and mass-spectrometry analysis time. However, other authors have pointed out the special merits of
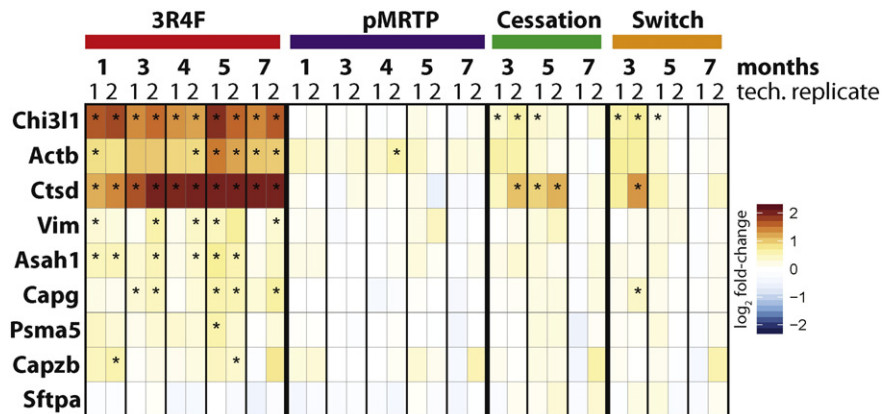

Fig. 5. Reverse-phase protein array (RPPA) results for selected core cluster components. RPPA result heatmap with target proteins in rows and exposure comparisons in columns. Results of two technical replicates are included and labeled correspondingly. The fold-change in each exposure group compared with the sham group at the same time point is color-coded (see color key) and statistically significant differences are marked (* = fdr-adj. *p*-value < 0.05). Statistics based on *t*-test of log-transformed data; only comparisons with at least three not missing values per group are considered.

2D-PAGE approaches, especially as a top-down method to study effects on intact proteins [14].

In the present manuscript, we wanted to address the question of whether 2D-PAGE could complement LC-MS/MS-based proteomics within our systems toxicology assessment framework. To this end, we analyzed lung proteome alterations in a 7-month mouse CS inhalation study by both 2D-PAGE and an iTRAQ-based LC-MS/MS workflow. As already reported, the iTRAQ workflow was able to capture the extensive effects of cigarette smoke exposure on the lung, including the xenobiotic, oxidative stress, metabolic, and inflammatory responses [8,11]. Proteome profiling by 2D-PAGE reproduced the general response, especially the decreased effect of pMRTP aerosol compared with cigarette smoke exposure and the lack of response in the cessation and switching samples (Fig. 2) (see limitations below). While the number of identified differentially abundant proteins was much lower in the 2D-PAGE analysis than that determined by iTRAQ, the response to cigarette smoke exposure detected by both proteomics methods clearly overlapped (Fig. 3). In summary, we can draw similar conclusions as in previous studies [16]: 2D-PAGE has a lower sensitivity for the detection of differentially abundant proteins as compared to iTRAQ, but it is complementary by confirming (and partially extending) the iTRAQ results.

Given the difference in the numbers of differentially abundant proteins identified by 2D-PAGE and iTRAQ, the question arose of how to best leverage both data types to support biological interpretation. For this, we employed a functional network embedding approach, in which the 2D-PAGE results were included in the observed effects on functional clusters that were defined mostly based on the iTRAQ results (Fig. 4). By this approach, the 2D-PAGE results further supported an induction by cigarette smoke exposure of immune (myeloid)-, surfactant-, proteasome-, and actin cytoskeleton-related processes. The biological relevance of the induced immune response and surfactants has been already discussed based on the iTRAQ data [8, 11], but the effects on the proteasome and actin cytoskeleton only became clearly apparent in this integrated analysis.

The proteasome cluster consisted of several proteasome components detected as upregulated upon CS exposure in the iTRAQ analysis and supported by the upregulated Psmd9 component in the 2D-PAGE analysis. One possibility is that this observation is related to the induced immune response upon CS exposure, because the proteasome plays an important role in antigen processing, e.g., by macrophages [35]. Of note, the proteasome cluster included Psmb10 (Mecl-1), a component of the immuno-proteasome. Alternatively or in addition, the upregulation of proteasome components could also play a more direct role, e.g., by supporting the degradation of proteins damaged upon CS exposure. For example, the stress response regulator Nrf2 has been implicated in the regulation of proteasome components upon CS exposure [36]. Functionally, it has been found that interference with the proteasome system increases emphysema susceptibility in mice [37]. Interestingly, upon acute/short-term exposure, CS impairs proteasome function [38,39], which might trigger a compensatory increase in the expression of proteasome components under chronic exposure conditions. Overall, several links between CS exposure and the proteasome have been established and we agree with Meiners et al. that it will be pertinent to further investigate the role of the proteasome and its regulation in lung diseases and long-term and sustained adaptation to chronic challenges, e.g., from CS exposure [40].

The integrated analysis of the effects of CS exposure by 2D-PAGE and iTRAQ also clearly implicated upregulation of actin cytoskeleton components in the response of lung tissue (Fig. 4). For example, upregulation of Capg (actin filament capping protein) and Efhd2 (a cytoskeletal adaptor protein) was supported by both methods, and 2D-PAGE complemented the iTRAQ results by providing evidence for the upregulation of Actb (beta actin), Capzb (actin filament capping protein) and Arhgdia (rho GDP dissociation inhibitor) upon CS exposure. Similar to the induction of proteasome components, the upregulation of these cytoskeleton components could reflect the CS-triggered immune-

response, which is associated with a higher motility state of activated immune cells (e.g., [41]). However, several studies also reported more specific effects of CS on the actin cytoskeleton. For example, CS modulated the actin cytoskeleton of an airway epithelium cell line [42], cigarette smoke condensate induced reorganization of the actin cytoskeleton in human bronchial epithelial cells [43], and treatment of human endothelial cells with cigarette smoke extract resulted in the reorganization of the actin cytoskeleton [44], and such alterations have been implicated in the maintenance of epithelial and endothelial barrier functions to counteract inflammatory processes in CS-exposed lungs [45]. The effect observed here on the actin cytoskeleton likely reflects relevant short- and/or long-term adaptive changes in response to CS exposure in the lung tissue, which will be interesting to investigate in more cellular and molecular detail in the future.

4.1. Scope and limitations of this study

The current article was focused on the question of what additional information the 2D-PAGE approach can add for the analysis of proteome alterations in the context of a systems toxicology study. The reader is referred to the publications by Phillips et al. [8] and Titz et al. [11] for a broader discussion of the biological/toxicological conclusions, especially for the comparison of CS and pMRTP exposure and cessation/switching across all measured endpoints. Here, — in addition to the general response patterns between the groups – we especially focused on the last time point of CS exposure, which showed the highest number of differentially abundant proteins for the 2D-PAGE approach. Due to its higher variability compared to the iTRAQ approach (Supplementary Fig. 1), the 2D-PAGE approach would especially benefit from a larger number of replicates in future studies. In addition, the number of identified proteins could be increased by analyzing the samples on large format gels (18 cm and 24 cm) and by performing LC separation of the tryptic peptides. Further study of the effects of different switching/cessation timepoints and of the overall length of the study could yield additional insights. For example, for the 2-month switching/cessation time point, which was chosen based on a previous inhalation study [17], the majority of 3R4F-related changes became significantly attenuated within 3 months of cessation or switching and some of the end points were as low as the sham at months 5 and 7 [8,11]. In future studies, inclusion of later switching/cessation time points might reveal markers both of the reversible, adaptive response as well as of permanent tissue damage.

4.2. Conclusions

Within our systems toxicology framework, we have analyzed the effects of cigarette smoke and pMRTP aerosol exposure on the mouse lung proteome both by 2D-PAGE and using an iTRAQ workflow. Consistent with previous comparisons (e.g., [16]), the iTRAQ workflow clearly provided greater coverage of the CS-induced effects. Nevertheless, the 2D-PAGE/MALDI MS/MS results proved usefulness to support the overall trends, especially the lower effect of pMRTP aerosol than CS on the lung proteome, and the CS effect on specific functional categories such as actin cytoskeleton regulation. While the field of toxicoproteomics is employing more and more gel-free methods (labeled and label-free), robust 2D-PAGE retains a role as a complementary method for intact proteins.

Supplementary data to this article can be found online at http://dx.doi.org/10.1016/j.jprot.2016.05.037.

Declaration of interest

Transparency document

The Transparency document associated with this article can be found in the online version.

Acknowledgements

References

[1] Family Smoking Prevention and Tobacco Control Act (FSPTCA), Public Law No. 111–312009.
[2] R.R. Baker, Smoke generation inside a burning cigarette: modifying combustion to develop cigarettes that may be less hazardous to health, Prog. Energy Combust. Sci. 32 (4) (2006) 373–385.
[3] M. Borgerding, J. Bodnar, H. Chung, P. Mangan, C. Morrison, C. Risner, J. Rogers, D. Simmons, M. Uhrig, F. Wendelboe, Chemical and biological studies of a new cigarette that primarily heats tobacco: part 1. Chemical composition of mainstream smoke, Food Chem. Toxicol. 36 (3) (1998) 169–182.
[4] K. Torikaiu, Y. Uwano, T. Nakamori, W. Tarora, H. Takahashi, Study on tobacco components involved in the pyrolytic generation of selected smoke constituents, Food Chem. Toxicol. 43 (4) (2005) 559–568.
[5] M.K. Schorp, A.R. Tricker, R. Dempsey, Reduced exposure evaluation of an electrically heated cigarette smoking system. Part 1: non-clinical and clinical insights, Regul. Toxicol. Pharmacol. 64 (2) (2012) S1–S10.
[6] M. Forster, C. Liu, M.G. Duke, K.G. McAdam, C.J. Proctor, An experimental method to study emissions from heated tobacco between 100–200 °C, Chem. Cent. J. 9 (2015) 20.
[7] B. Phillips, E. Veljkovic, S. Boue, W.K. Schlage, G. Vuillaume, F. Martin, B. Titz, P. Leroy, A. Buettner, A. Elamin, A. Oviedo, M. Cabanski, E. Guedj, T. Schneider, M. Talikka, N.V. Ivanov, P. Vanscheeuwijck, M.C. Peitsch, J. Hoeng, An 8-month systems toxicology inhalation/cessation study in Apoe−/− mice to investigate cardiovascular and respiratory Exposure effects of a candidate modified risk tobacco product, THS 2.2, compared with conventional cigarettes, Toxicol. Sci. 149 (2) (2016) 411–432.
[8] B. Phillips, E. Veljkovic, M.J. Peck, A. Buettner, A. Elamin, E. Guedj, G. Vuillaume, N.V. Ivanov, F. Martin, S. Boué, W.K. Schlage, T. Schneider, B. Titz, M. Talikka, P. Vanscheeuwijck, J. Hoeng, A 7-month cigarette smoke inhalation study in C57BL/6 mice demonstrates reduced lung inflammation and emphysema following smoking cessation or aerosol exposure from a prototypic modified risk tobacco product, Food Chem. Toxicol. 80 (2015) 328–345.
[9] U. Kogel, W.K. Schlage, F. Martin, Y. Xiang, S. Ansari, P. Leroy, P. Vanscheeuwijck, S. Gebel, A. Buettner, C. Wyss, M. Esposito, J. Hoeng, M.C. Peitsch, A 28-day rat inhalation study with an integrated molecular toxicology endpoint demonstrates reduced exposure effects for a prototypic modified risk tobacco product compared with conventional cigarettes, Food Chem. Toxicol. 68 (2014) 204–217.
[10] S.J. Sturla, A.R. Boobis, R.E. FitzGerald, J. Hoeng, R.J. Kavlock, K. Schirmer, M. Whelan, M.F. Wilks, M.C. Peitsch, Systems toxicology: from basic research to risk assessment, Chem. Res. Toxicol. 27 (3) (2014) 314–329.
[11] B. Titz, S. Boue, B. Phillips, M. Talikka, T. Vihervaara, T. Schneider, C. Nury, A. Elamin, E. Guedj, M.J. Peck, W.K. Schlage, M. Cabanski, P. Leroy, G. Vuillaume, F. Martin, N.V. Ivanov, E. Veljkovic, K. Ekroos, R. Laaksonen, P. Vanscheeuwijck, M.C. Peitsch, J. Hoeng, Effects of cigarette smoke, cessation and switching to two heat-not-burn tobacco products on lung lipid metabolism in C57BL/6 and Apoe−/− mice - an integrative systems toxicology analysis, Toxicol. Sci. 149 (2) (2016) 441–457.
[12] B. Titz, A. Elamin, F. Martin, T. Schneider, S. Dijon, N.V. Ivanov, J. Hoeng, M.C. Peitsch, Proteomics for systems toxicology, Comput. Struct. Biotechnol. J. 11 (18) (2014) 73–90.
[13] B. Titz, T. Schneider, A. Elamin, F. Martin, S. Dijon, N. Ivanov, J. Hoeng, M. Peitsch, Analysis of proteomic data for toxicological applications, Computational Systems Toxicology, Springer, New York 2015, pp. 257–284.
[14] G. Arentz, F. Weiland, M.K. Oehler, P. Hoffmann, State of the art of 2D DIGE, Proteomics Clin. Appl. 9 (3–4) (2015) 277–288.
[15] T. Rabilloud, P. Lescuyer, Proteomics in mechanistic toxicology: history, concepts, achievements, caveats, and potential, Proteomics 15 (5–6) (2015) 1051–1074.
[16] S.M. Pütz, A.M. Boehm, T. Stiewe, A. Sickmann, iTRAQ analysis of a cell culture model for malignant transformation, including comparison with 2D-PAGE and SILAC, J. Proteome Res. 11 (4) (2012) 2140–2153.
[17] J. Hoeng, M. Talikka, F. Martin, A. Sewer, X. Yang, A. Iskandar, W.K. Schlage, M.C. Peitsch, Case study: the role of mechanistic network models in systems toxicology, Drug Discov. Today 19 (2) (2014) 183–192.
[18] S. Ansari, K. Baumer, S. Boue, S. Dijon, R. Dulize, K. Ekroos, A. Elamin, C. Foong, E. Guedj, J. Hoeng, N.V. Ivanov, S. Krishnan, P. Leroy, F. Martin, C. Merg, M.J. Peck, M.C. Peitsch, B. Phillips, W.K. Schlage, T. Schneider, M. Talikka, B. Titz, P. Vanscheeuwijck, E. Veljkovic, T. Vihervaara, G. Vuillaume, C.Q. Woon, Comprehensive systems biology analysis of a 7-month cigarette smoke inhalation study in C57BL/6 mice, Scientific Data 3 (2016) 150077.
[19] R.C. Gentleman, V.J. Carey, D.M. Bates, B. Bolstad, M. Dettling, S. Dudoit, B. Ellis, L. Gautier, Y. Ge, J. Gentry, Bioconductor: open software development for computational biology and bioinformatics, Genome Biol. 5 (10) (2004) R80.
[20] M. Pawlak, E. Schick, M.A. Bopp, M.J. Schneider, P. Oroszlan, M. Ehrat, Zeptosens' protein microarrays: a novel high performance microarray platform for low abundance protein analysis, Proteomics 2 (4) (2002) 383–393.
[21] L. Väremo, J. Nielsen, I. Nookaew, Enriching the gene set analysis of genome-wide data by incorporating directionality of gene expression and combining statistical hypotheses and methods, Nucleic Acids Res. 41 (8) (2013) 4378–4391.
[22] D. Szklarczyk, A. Franceschini, S. Wyder, K. Forslund, D. Heller, J. Huerta-Cepas, M. Simonovic, A. Roth, A. Santos, K.P. Tsafou, M. Kuhn, P. Bork, L.J. Jensen, C. von Mering, STRING v10: protein-protein interaction networks, integrated over the tree of life, Nucleic Acids Res. 43 (Database issue) (2015) D447–D452.
[23] M. Rosvall, C. Bergstrom, Maps of information flow reveal community structure in complex networks, arXiv preprint physics.soc-ph/0707.0609, 2007.
[24] J. Chen, E.E. Bardes, B.J. Aronow, A.G. Jegga, ToppGene suite for gene list enrichment analysis and candidate gene prioritization, Nucleic Acids Res. 37 (Web Server issue) (2009) W305–W311.
[25] J.A. Vizcaíno, E.W. Deutsch, R. Wang, A. Csordas, F. Reisinger, D. Ríos, J.A. Dianes, Z. Sun, T. Farrah, N. Bandeira, ProteomeXchange provides globally coordinated proteomics data submission and dissemination, Nat. Biotechnol. 32 (3) (2014) 223–226.
[26] P. Flecknell, Replacement, reduction and refinement, ALTEX 19 (2) (2002) 73–78.
[27] M.E. Burczynski, M. McMillian, J. Ciervo, L. Li, J.B. Parker, R.T. Dunn 2nd, S. Hicken, S. Farr, M.D. Johnson, Toxicogenomics-based discrimination of toxic mechanism in HepG2 human hepatoma cells, Toxicol. Sci. 58 (2) (2000) 399–415.
[28] E.F. Nuwaysir, M. Bittner, J. Trent, J.C. Barrett, C.A. Afshari, Microarrays and toxicology: the advent of toxicogenomics, Mol. Carcinog. 24 (3) (1999) 153–159.
[29] S.U. Ruepp, R.P. Tonge, J. Shaw, N. Wallis, F. Pognan, Genomics and proteomics analysis of acetaminophen toxicity in mouse liver, Toxicol. Sci. 65 (1) (2002) 135–150.
[30] Y.-M. Go, J.R. Roede, M. Orr, Y. Liang, D.P. Jones, Integrated redox proteomics and metabolomics of mitochondria to identify mechanisms of Cd toxicity, Toxicol. Sci. 139 (1) (2014) 59–73.
[31] A. Wilmes, C. Bielow, C. Ranninger, P. Bellwon, L. Aschauer, A. Limonciel, H. Chassaigne, T. Kristl, S. Aiche, C.G. Huber, Mechanism of Cisplatin Proximal Tubule Toxicity Revealed by Integrating Transcriptomics, Proteomics, Metabolomics and Biokinetics, Toxicology In Vitro, 2014.
[32] J. Yuan, H. Gao, J. Sui, H. Duan, W.N. Chen, C.B. Ching, Cytotoxicity evaluation of oxidized single-walled carbon nanotubes and graphene oxide on human hepatoma HepG2 cells: an iTRAQ-coupled 2D LC-MS/MS proteome analysis, Toxicol. Sci. 126 (1) (2012) 149–161.
[33] R. Bruderer, O.M. Bernhardt, T. Gandhi, S.M. Miladinović, L.-Y. Cheng, S. Messner, T. Ehrenberger, V. Zanotelli, Y. Butscheid, C. Escher, Extending the limits of quantitative proteome profiling with data-independent acquisition and application to acetaminophen-treated three-dimensional liver microtissues, Mol. Cell. Proteomics 14 (5) (2015) 1400–1410.
[34] T. Rabilloud, P. Lescuyer, Proteomics in mechanistic toxicology: History, concepts, achievements, caveats, and potential, Proteomics 15 (5–6) (2015) 1051–1074.
[35] I.E. Keller, O. Vosyka, S. Takenaka, A. Kloss, B. Dahlmann, L.I. Willems, M. Verdoes, H.S. Overkleeft, E. Marcos, S. Adnot, S.M. Hauck, C. Ruppert, A. Gunther, S. Herold, S. Ohno, H. Adler, O. Eickelberg, S. Meiners, Regulation of immunoproteasome function in the lung, Sci. Rep. 5 (2015) 10230.
[36] D. Malhotra, R. Thimmulappa, N. Vij, A. Navas-Acien, T. Sussan, S. Merali, L. Zhang, S.G. Kelsen, A. Myers, R. Wise, R. Tuder, S. Biswal, Heightened endoplasmic reticulum stress in the lungs of patients with chronic obstructive pulmonary disease: the role of Nrf2-regulated proteasomal activity, Am. J. Respir. Crit. Care Med. 180 (12) (2009) 1196–1207.
[37] Y. Yamada, U. Tomaru, A. Ishizu, T. Ito, T. Kiuchi, A. Ono, S. Miyajima, K. Nagai, T. Higashi, Y. Matsuno, H. Dosaka-Akita, M. Nishimura, S. Miwa, M. Kasahara, Decreased proteasomal function accelerates cigarette smoke-induced pulmonary emphysema in mice, Lab. Investig. 95 (6) (2015) 625–634.
[38] S.H. van Rijt, I.E. Keller, G. John, K. Kohse, A.O. Yildirim, O. Eickelberg, S. Meiners, Acute cigarette smoke exposure impairs proteasome function in the lung, Am. J. Physiol. Lung Cell. Mol. Physiol. 303 (9) (2012) L814–L823.
[39] A. Somborac-Bacura, M. van der Toorn, L. Franciosi, D.J. Slebos, T. Zanic-Grubisic, R. Bischoff, A.J. van Oosterhout, Cigarette smoke induces endoplasmic reticulum stress response and proteasomal dysfunction in human alveolar epithelial cells, Exp. Physiol. 98 (1) (2013) 316–325.
[40] S. Meiners, I.E. Keller, N. Semren, A. Caniard, Regulation of the proteasome: evaluating the lung proteasome as a new therapeutic target, Antioxid. Redox Signal. 21 (17) (2014) 2364–2382.
[41] J. Monypenny, H.C. Chou, I. Banon-Rodriguez, A.J. Thrasher, I.M. Anton, G.E. Jones, Y. Calle, Role of WASP in cell polarity and podosome dynamics of myeloid cells, Eur. J. Cell Biol. 90 (2–3) (2011) 198–204.
[42] D. Olivera, C. Knall, S. Boggs, J. Seagrave, Cytoskeletal modulation and tyrosine phosphorylation of tight junction proteins are associated with mainstream cigarette smoke-induced permeability of airway epithelium, Exp. Toxicol. Pathol. 62 (2) (2010) 133–143.
[43] C.A. Carter, J.T. Hamm, Multiplexed quantitative high content screening reveals that cigarette smoke condensate induces changes in cell structure and function through alterations in cell signaling pathways in human bronchial cells, Toxicology 261 (3) (2009) 89–102.
[44] B.H. Lin, M.H. Tsai, C.K. Lii, T.S. Wang, IP3 and calcium signaling involved in the reorganization of the actin cytoskeleton and cell rounding induced by cigarette smoke extract in human endothelial cells, Environ. Toxicol. (2015).
[45] K.S. Schweitzer, H. Hatoum, M.B. Brown, M. Gupta, M.J. Justice, B. Beteck, M. Van Demark, Y. Gu, R.G. Presson Jr., W.C. Hubbard, I. Petrache, Mechanisms of lung endothelial barrier disruption induced by cigarette smoke: role of oxidative stress and ceramides, Am. J. Physiol. Lung Cell. Mol. Physiol. 301 (6) (2011) L836–L846.